Respiratory Research and Treatment

https://rrt.cultechpub.com/rrt

Cultech Publishing

Article

Mitochondrial Bioenergetic Remodeling Associated with LCRMP-1 Expression in Lung Adenocarcinoma

Syed Luqman Ali[1,*], Muhammad Fawad[2]

[1]Department of Biochemistry, Abdul Wali Khan University, Mardan, Pakistan

[2]Department of Zoology, Islamia College, Peshawar, Pakistan

[*]Corresponding author: Syed Luqman Ali, syedluqmanali5@gmail.com

Abstract

Lung adenocarcinoma, the most common subtype of non-small cell lung cancer (NSCLC), is marked by metabolic reprogramming and mitochondrial dysregulation. Long-form collapsin response mediator protein-1 (LCRMP-1) is implicated in tumor progression, but its role in mitochondrial transcriptional regulation remains unclear. Using publicly available microarray data (GSE308874) from lung adenocarcinoma cell lines with LCRMP-1 overexpression or silencing, differentially expressed genes (DEGs) were identified, and mitochondrial-associated genes were analyzed via Gene Ontology (GO), kyoto encyclopedia of genes and genomes (KEGG) enrichment, protein-protein interaction (PPI), co-expression, and network clustering. Transcriptomic factor enrichment and drug perturbation analyses were performed to uncover upstream regulators and therapeutic targets, and prognostic relevance was assessed using Kaplan-Meier survival analysis. LCRMP-1 modulation induced widespread transcriptomic changes, prominently affecting mitochondrial genes involved in oxidative phosphorylation (OXPHOS), respiration, redox balance, and metabolism. Network analysis revealed a core mitochondrial module including CYCS, NDUFAB1, TUFM, VDAC1, TOMM20, ETFA, SSBP1, and SUCLA2, regulated by PRDM2, MLX, E2F4, and HMGN3, with drug perturbation profiles indicating potential pharmacological interventions. Several mitochondrial genes, notably TUFM and CYCS, correlated significantly with patient survival. This integrative study highlights LCRMP-1-mediated mitochondrial reprogramming as a key feature of lung adenocarcinoma and identifies hub genes and regulators as potential biomarkers and therapeutic targets.

Keywords

Lung adenocarcinoma, LCRMP-1, Mitochondrial dysfunction, Transcriptomic analysis, Protein-protein interaction network, Prognostic biomarkers

Article History

Received: 13 December 2025 Revised: 08 February 2026

Accepted: 13 March 2026 Available Online: 18 March 2026

Graphical Abstract

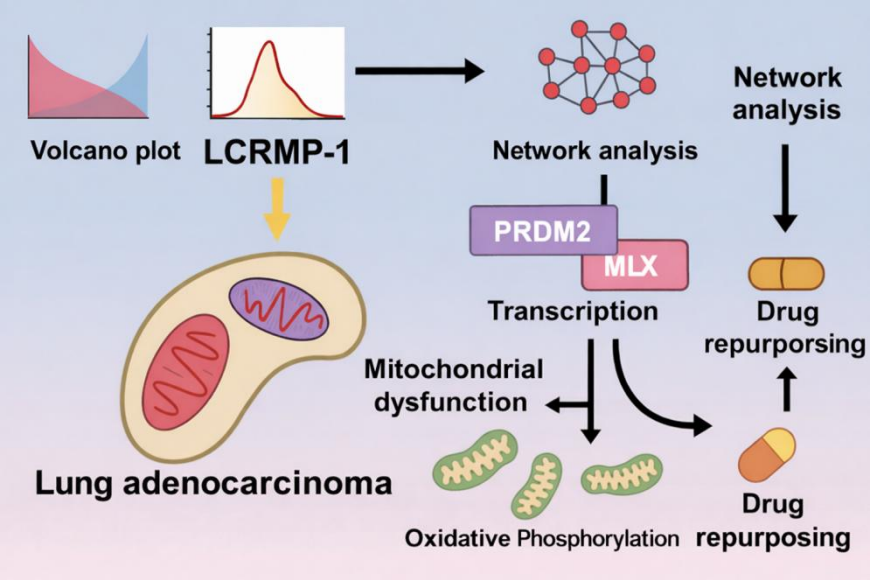

1. Introduction

Lung cancer continues to be the leading cause of cancer-related mortality worldwide, accounting for millions of deaths annually, with non-small cell lung cancer (NSCLC) representing the majority of cases. Among NSCLC subtypes, lung adenocarcinoma is the most prevalent and is characterized by remarkable molecular heterogeneity, aggressive tumor behavior, and a high propensity for metastasis [1]. Despite significant advances in early detection, targeted therapy, and immunotherapy, the overall survival of lung adenocarcinoma patients remains unsatisfactory. Therapeutic resistance and disease recurrence are common challenges, underscoring the need for a deeper understanding of the molecular mechanisms driving tumor progression and identifying novel prognostic and therapeutic targets [2].

Mitochondria are central regulators of cellular metabolism, energy homeostasis, and apoptotic signaling, and their dysregulation has been increasingly recognized as a hallmark of cancer. In tumor cells, mitochondrial bioenergetics are often rewired to meet the elevated demands for ATP production, biosynthesis, and redox balance, facilitating cancer cell survival and proliferation [3]. Alterations in mitochondrial gene expression, dynamics, and function have been associated with enhanced metastatic potential, chemoresistance, and poor clinical outcomes in lung adenocarcinoma. The ability of mitochondria to integrate metabolic signals with stress responses and apoptotic pathways makes them critical hubs for understanding cancer biology and identifying novel therapeutic vulnerabilities (Figure 1).

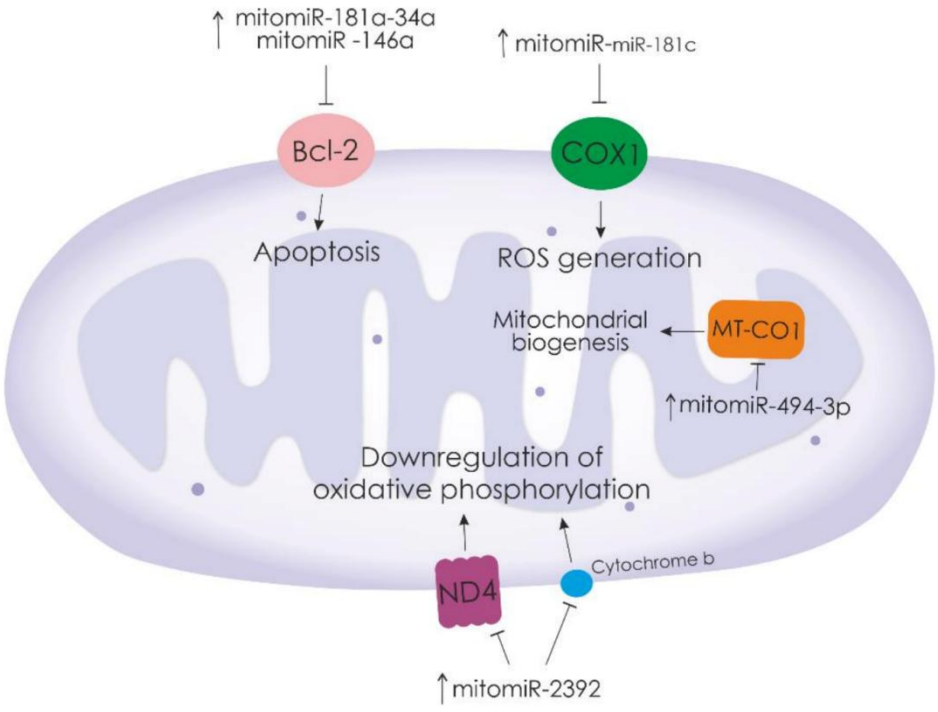

Figure 1. Mitochondrial miRNAs that regulate the expression of major mitochondrial proteins in Adenocarcinoma.

Long-form collapsin response mediator protein-1 (LCRMP-1) is a cytoskeleton-associated protein that has been implicated in promoting cancer cell invasion, migration, and metastasis. Previous studies have demonstrated that high LCRMP-1 expression correlates with poor prognosis in lung adenocarcinoma patients [4]. While its role in cytoskeletal remodeling and cell motility is well established, emerging evidence suggests that LCRMP-1 may also influence mitochondrial function and metabolic reprogramming, linking structural and bioenergetic adaptations in tumor cells. The precise mechanisms by which LCRMP-1 regulates mitochondrial gene expression and function, however, remain largely unexplored. Integrative transcriptomic and network-based analyses provide a powerful framework for elucidating complex molecular regulatory mechanisms in cancer [5]. By combining differential gene expression analysis with pathway enrichment, protein-protein interaction (PPI) networks, gene co-expression analysis, and upstream transcription factor (TF) identification, it is possible to map functional modules that orchestrate key aspects of tumor biology. Leveraging pharmacological perturbation datasets enables the identification of candidate drugs that can target these networks, offering translational relevance for therapeutic development [6].

In the present study, we applied a comprehensive transcriptomic approach to investigate the impact of LCRMP-1 on mitochondrial gene expression in lung adenocarcinoma. Using publicly available microarray data, we identified differentially expressed mitochondrial genes and characterized their functional roles through Gene Ontology (GO) and kyoto encyclopedia of genes and genomes (KEGG) pathway enrichment analyses [7]. PPI and co-expression network analyses were conducted to uncover central hub genes and key mitochondrial modules, while upstream TF and potential pharmacological modulators were explored through integrated enrichment analyses. Finally, the prognostic significance of prioritized mitochondrial genes was assessed in lung adenocarcinoma patient cohorts. This integrative study provides novel insights into LCRMP-1-mediated mitochondrial reprogramming, highlights mitochondrial hub genes as potential biomarkers, and offers a foundation for identifying therapeutic strategies targeting mitochondrial vulnerabilities in lung adenocarcinoma.

2. Methods and Materials

2.1 Data Retrieval and Dataset Selection

Publicly available transcriptomic data were obtained from the NCBI Gene Expression Omnibus (GEO) under accession number GSE308874, which contains microarray-based gene expression profiles of human lung adenocarcinoma cell lines Human lung adenocarcinoma cell line CL1-0 (CL1-0) and Human lung adenocarcinoma cell line CL1-5 (CL1-5) with experimentally manipulated LCRMP-1 expression [8]. The dataset includes CL1-0 cells overexpressing LCRMP-1 using two independent clones compared with vector control cells, as well as CL1-5 cells with LCRMP-1 silencing compared with scramble control cells, with each experimental condition generated using two biological replicates. Gene expression profiling was performed using the Phalanx Human OneArray Ver. 6 Release 1 platform (GPL16951). Raw expression data and associated metadata were downloaded from the GEO repository, and sample annotations were verified using Series Matrix and MINiML files. Standard preprocessing and quality control procedures appropriate for one-color microarray data were applied, including background correction and normalization, to minimize technical variation and enable reliable comparison of gene expression across experimental groups.

Differential gene expression analysis was conducted in R (version 4.3.1) using the limma package (version 3.56.2), with background-corrected and quantile-normalized one-color microarray data; linear models were fitted using default settings, and statistical significance was determined using Benjamini-Hochberg false discovery rate (FDR) correction, with adjusted $P < 0.05$ considered significant. Probe-to-gene mapping was performed using the GPL16951 platform annotation file provided by GEO.

2.2 Identification of Differentially Expressed Genes (DEGs)

Differential expression analysis was conducted using the normalized microarray expression data obtained from the GSE308874 dataset. Samples were assigned to cancer and normal groups based on the GEO-provided annotations. Gene expression values were log2 transformed where appropriate, and probes were mapped to corresponding gene symbols using the platform annotation file (GPL16951), with probes lacking valid gene annotations excluded from further analysis. Statistical comparisons between groups were performed using a linear modeling approach suitable for microarray data, and P values were adjusted for multiple testing using the Benjamini-Hochberg FDR method. Genes meeting the predefined significance criteria of adjusted P value < 0.05 were considered differentially expressed. Visualization of the analysis was carried out using volcano plots, mean-difference (MA) plots, boxplots, and expression density plots to assess data distribution, normalization performance, and analytical robustness.

2.3 Retrieval of Regulated Mitochondrial Genes

To specifically examine mitochondrial involvement at the transcriptional level, an additional gene-filtering strategy was applied focusing on mitochondrial-associated genes. A curated reference list of human mitochondrial genes was obtained from established mitochondrial databases and GO resources related to mitochondrial localization and function. Following differential expression analysis, gene identifiers were standardized and intersected with the mitochondrial gene reference set to extract genes linked to mitochondrial structure, metabolism, and signalling [9]. This approach

enabled the systematic identification of mitochondrial-related genes within the broader expression dataset while maintaining analytical rigor and reproducibility. Given the central role of mitochondria in cellular energy production, redox homeostasis, apoptosis, and metabolic reprogramming, focusing on mitochondrial genes provides a biologically relevant framework for understanding transcriptional alterations associated with cancer progression and cellular phenotypic changes.

2.4 Pathways Enrichment Analysis

GO and KEGG pathway enrichment analyses were performed to systematically characterize the functional attributes of the selected gene set [10]. GO analysis was conducted to annotate genes across the three standard domains: Biological Process (BP), Molecular Function (MF), and Cellular Component (CC). Enrichment analysis was carried out using a curated annotation database, and statistically overrepresented GO terms were identified by comparing the input gene list against an appropriate background gene set. Multiple testing correction was applied using the Benjamini-Hochberg FDR method, and adjusted p values below a predefined threshold were considered statistically significant. Enrichment scores were calculated as $-\log_{10}$ (p value) to facilitate comparative visualization across categories.

KEGG pathway enrichment analysis was performed to identify significantly overrepresented signaling and metabolic pathways associated with the gene set. Genes were mapped to KEGG pathway identifiers, and pathway overrepresentation was assessed using a hypergeometric or equivalent statistical test. Similar to GO analysis, multiple hypothesis testing correction was applied to control the FDR [11], and significantly enriched pathways were selected based on adjusted p value criteria. The enrichment results from both GO and KEGG analyses were visualized using appropriate graphical representations, including dot plots and network-based diagrams, to enable systematic interpretation of functional patterns within the dataset [12]. Mitochondrial gene filtering was performed by intersecting DEGs with curated mitochondrial gene sets derived from GO mitochondrial terms and published mitochondrial databases. GO (BP, CC, MF) and KEGG pathway enrichment analyses were carried out using clusterProfiler (version 4.8.3) with default hypergeometric testing, FDR correction enabled, minimum gene count set to 2, and q-value cutoff of 0.05; enrichment scores were calculated as -log10 (p-value).

2.5 Protein-Protein Interaction Network

PPI analysis was performed using the list of highly differentially expressed mitochondrial genes as input. Experimentally validated and predicted interactions were retrieved from a curated PPI database and assembled into an interaction network [13]. The network was visualized and analyzed using network analysis software to assess topological properties, including node degree and connectivity, enabling the identification of highly connected hub proteins. A refined subnetwork was extracted based on interaction density to highlight core functional modules, and genes were prioritized by integrating differential expression metrics with network centrality measures, resulting in the selection of the top 10 mitochondrial genes for downstream analysis [14].

PPI networks were constructed using STRING database (version 11.5) with a minimum interaction confidence score of 0.4, and networks were visualized and analyzed in Cytoscape (version 3.10.1) using node degree and connectivity for hub gene identification.

2.6 Genes Co-expression

Gene co-expression analysis was performed using the prioritized mitochondrial genes to evaluate coordinated expression patterns. Gene expression correlation data were retrieved from a curated co-expression database, integrating experimentally observed co-expression in Homo sapiens and inferred co-expression transferred from orthologous genes in other organisms. Pairwise gene-gene associations were computed based on correlation strength, and significant co-expression relationships were visualized as triangular heatmap matrices. Cross-species conservation of co-expression was assessed by mapping orthologous relationships, enabling identification of evolutionarily conserved transcriptional modules among mitochondrial genes [15]. Network clustering was performed using the MCODE plugin (version 2.0.2) with default parameters (degree cutoff = 2, node score cutoff = 0.2, K-core = 2). Gene co-expression analysis was performed using STRING co-expression channels and all RNA-seq and chromatin immunoprecipitation sequencing (ChIP-seq) sample and signature search all RNA-seq and ChIP-seq sample and signature search (ARCHS4) (2024 release), with Pearson correlation-based associations and cross-species transferred co-expression enabled. TF enrichment analysis integrated datasets from encyclopedia of DNA elements (ENCODE) (2023 release), ReMap (2024), and genotype-tissue expression (GTEx) v8, using default enrichment thresholds.

2.7 Integrated Network and Clustering Analysis

An integrated network and clustering analysis was conducted using the prioritized mitochondrial genes to identify key functional modules. PPI data were retrieved from a curated interaction database and imported into network analysis software [16]. The network was clustered using a topology-based clustering algorithm to define densely connected gene modules, with nodes grouped according to shared interaction patterns. Cluster composition, connectivity, and centrality measures were evaluated to identify hub genes with active roles in mitochondrial function. Genes exhibiting high intra-

cluster connectivity and strong interaction density were prioritized, resulting in the identification of eight core mitochondrial genes for downstream interpretation [17].

2.8 Transcriptomic Factor and Drug Therapeutics

Transcriptomic factor and drug-perturbation analyses were performed using a multi-database enrichment framework. The input gene signature was first subjected to TF enrichment analysis by integrating co-expression resources (ARCHS4 and GTEx) with chromatin immunoprecipitation datasets from ENCODE, ReMap, and literature-curated ChIP-seq repositories to identify putative upstream regulators. Drug-gene expression associations were then evaluated using DrugMatrix [18] to assess *in vivo* toxicogenomic perturbation profiles, the Proteomics Drug Atlas (2023) to capture drug-induced protein-level changes, and Sciplex Drug Perturbation Signatures (2025) to analyze single-cell transcriptional responses across multiple cell lines, doses, and time points. Enrichment scores and directional regulation were computed for each dataset, and statistically significant overlaps between the query signature and perturbation profiles were aggregated to generate an integrated regulatory and pharmacological interaction map. Drug perturbation analyses were conducted using DrugMatrix, Proteomics Drug Atlas (2023), and Sciplex Drug Perturbation Signatures (2025) with default enrichment and overlap scoring parameters.

2.9 Survival and Prognostic Analysis

A Kaplan-Meier survival analysis was performed to evaluate the prognostic relevance of selected mitochondrial and metabolic genes in lung adenocarcinoma [19]. Gene-specific Affymetrix probe IDs were queried using the KM Plotter platform, restricting analyses to overall survival and applying median expression values to dichotomize patients into high- and low-expression cohorts [20]. Default settings were maintained for clinical covariates, including histology, tumor stage, grade, American joint committee on cancer (AJCC) classifications, treatment history, and smoking status, ensuring an unbiased and inclusive dataset. Median expression cutoffs were computed using user-selected probe sets, with censored samples retained according to platform guidelines. Array quality controls were applied to exclude biased datasets. The platform generated Kaplan-Meier curves [21], hazard metrics, and median survival estimates for each gene, which were subsequently compiled for comparative interpretation and downstream biomarker selection. Survival and prognostic analyses were performed using the Kaplan-Meier Plotter online tool (accessed January 2025) with median expression cutoffs, overall survival as the endpoint, auto-selected Affymetrix probe sets, and default clinical covariate settings.

3. Results

3.1 Data Retrieval and Dataset Selection

Analysis of the GSE308874 dataset revealed that modulation of LCRMP-1 expression induced distinct and consistent transcriptomic changes in lung adenocarcinoma cells. In CL1-0 cells, overexpression of LCRMP-1 in both independent clones resulted in concordant alterations in gene expression compared with vector controls, indicating robust effects attributable to LCRMP-1 rather than clonal variation. Conversely, silencing of LCRMP-1 in CL1-5 cells led to an opposing expression pattern relative to scramble controls, further supporting a regulatory role for LCRMP-1. Differential expression analysis identified a subset of genes that were consistently upregulated upon LCRMP-1 overexpression and downregulated upon LCRMP-1 knockdown, many of which are functionally associated with angiogenesis, transcriptional regulation, and cancer-related signaling pathways. These reciprocal expression trends across gain- and loss-of-function models suggest that LCRMP-1 acts as a transcriptional co-regulator that promotes angiogenic and pro-tumorigenic gene programs in lung adenocarcinoma cells.

3.2 Identification of DEGs

Differential expression analysis of the GSE308874 microarray dataset identified a substantial number of DEGs between cancer and normal conditions using an adjusted P value threshold of < 0.05. As shown in the volcano plot (Figure 2A), numerous genes exhibited significant expression changes, with clearly separated clusters of upregulated genes (red) and downregulated genes (blue), indicating robust transcriptional differences between the two groups. The magnitude and statistical significance of these changes suggest widespread dysregulation of gene expression associated with the cancer phenotype. Consistently, the MA plot (Figure 2B) demonstrated a broad distribution of log2 fold changes across the range of expression values, with both highly expressed and moderately expressed genes contributing to the pool of DEGs, further supporting the reliability of the differential expression results. Quality assessment of the normalized data showed comparable expression distributions across all samples, as evidenced by the boxplots (Figure 2C), indicating effective normalization and minimal technical bias. In addition, the expression density plots (Figure 2D) revealed highly overlapping intensity distributions between cancer and normal samples, confirming overall data consistency while still allowing for distinct gene-level expression differences. Together, these analyses confirm the successful identification of DEGs and provide a solid foundation for downstream functional and pathway enrichment analyses.

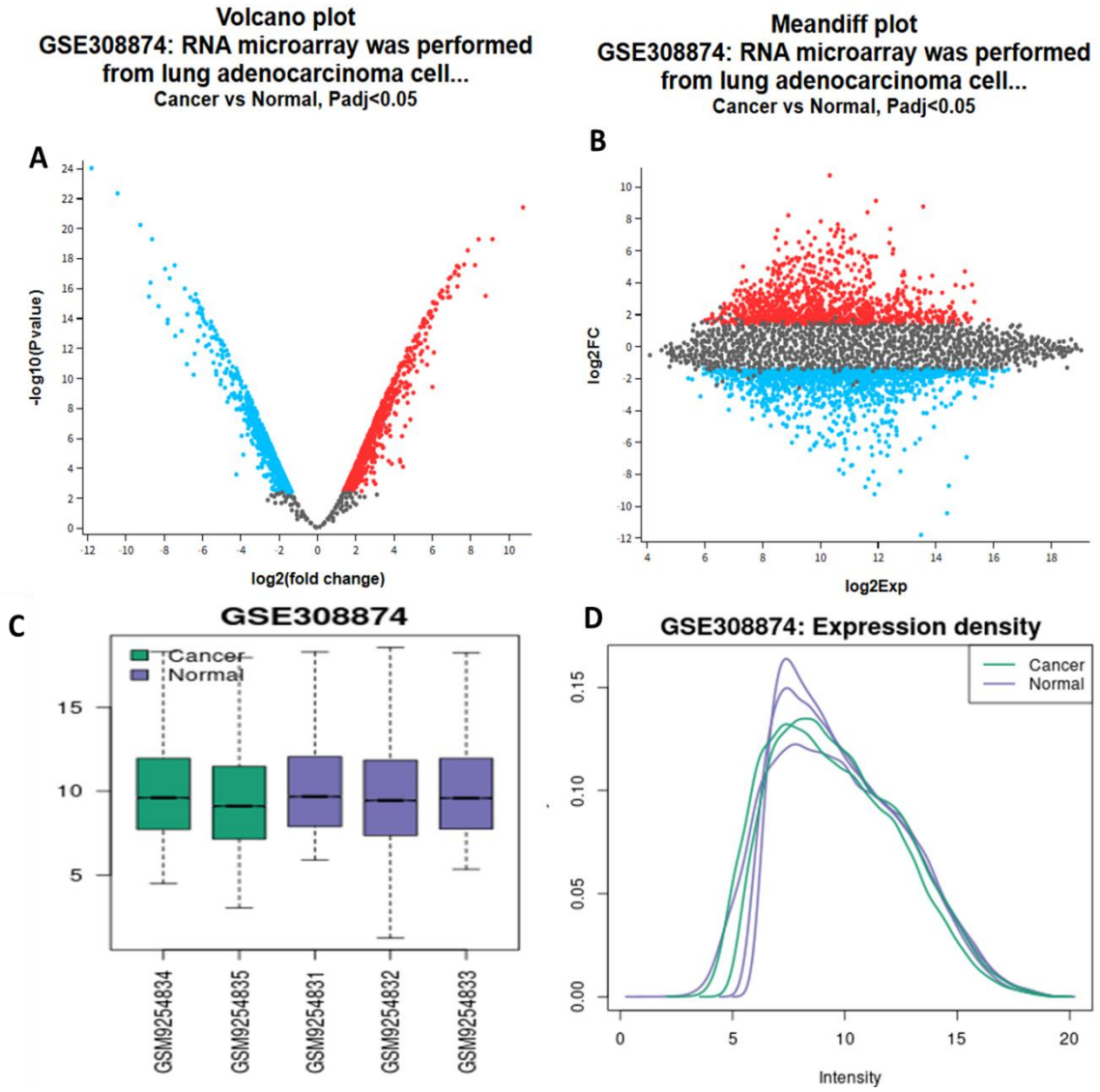

Figure 2. Identification of DEGs in GSE308874, showing volcano plot, mean-difference plot (MA plot), boxplots of normalized expression values, and expression density distributions between cancer and normal samples (adjusted $P < 0.05$).

3.3 Retrieval of Regulated Mitochondrial Genes

A comprehensive screening of the differentially expressed gene dataset was performed to identify genes associated with mitochondrial structure and function. By intersecting the list of DEGs with curated mitochondrial gene annotations obtained from established mitochondrial gene resources, a total of 983 mitochondrial-related genes were retrieved from the dataset. These genes represent a broad spectrum of mitochondrial processes, including oxidative phosphorylation (OXPHOS), energy metabolism, mitochondrial biogenesis, and regulation of apoptotic signaling. The identification of this large subset of regulated mitochondrial genes indicates that mitochondrial pathways are extensively involved in the transcriptional alterations observed in the dataset and provides a focused gene set for subsequent functional enrichment and mechanistic analyses [22].

3.4 Pathways Enrichment Analysis

Pathway enrichment analysis was performed to functionally characterize the regulated mitochondrial genes and to identify BP disproportionately represented within this gene set. GO-based enrichment focusing on BP was used to evaluate the involvement of mitochondrial genes in cellular metabolism, respiration, and energy production. Enrichment significance was assessed using adjusted P values, and pathways were ranked according to enrichment scores and gene counts. This approach enabled systematic identification of mitochondrial pathways potentially impacted at the transcriptional level and provided biological context for interpreting mitochondrial gene regulation in the dataset [23].

The BP enrichment results revealed that mitochondrial-related pathways were predominantly associated with cellular respiration, aerobic respiration, and electron transport chain (ETC) activity, as visualized by both the chord diagram and dot plot. The chord diagram illustrates extensive gene-pathway connectivity, highlighting coordinated regulation across multiple mitochondrial processes, including energy derivation by oxidation of organic compounds and generation of

precursor metabolites and energy. The dot plot further demonstrates that these pathways exhibit high enrichment scores and large gene counts, with particularly strong significance observed for cellular respiration and aerobic respiration [24]. Additional enriched terms related to mitochondrial transport, gene expression, translation, and respiratory chain complex assembly emphasize widespread modulation of mitochondrial structure and function, underscoring the central role of mitochondrial bioenergetics in the analyzed condition (Figure 3). The top 10 BP enrichment results revealed in Table 1. The top 10 GO BP terms for descriptive ranking purposes, while the full enrichment statistics are shown in Figure 3.

Table 1. The q-values reflect global FDR adjustment across the complete GO output rather than recalculation within the truncated table. The term with p = 1.0 is not interpreted as significant and does not affect downstream analyses or conclusions. We have clarified this in the revised table caption.

ID	Description	Gene Ratio	BgRatio	P value	Q value	Gene ID	Count	Enrichment. Score	Fold. Enrichment
GO:0198738	cell-cell signaling by wnt	1/925	446/18723	1	0.837111134	SDHAF2	1	5.03826E-11	0.04538359
GO:0016055	Wnt signaling pathway	1/925	444/18723	1	0.837111134	SDHAF2	1	5.5897E-11	0.04558802
GO:0001667	ameboidal-type cell migration	3/925	475/18723	0.999999991	0.837111134	C1QBP/GPX1/SYNJ2BP	3	3.87182E-09	0.127838407
GO:0007409	axonogenesis	2/925	418/18723	0.999999988	0.837111134	AFG3L2/BCL2	2	5.00792E-09	0.096847278
GO:0007178	transmembrane receptor protein serine/threonine kinase signaling pathway	1/925	355/18723	0.999999987	0.837111134	FKBP8	1	5.6174E-09	0.05701713
GO:0032970	regulation of actin filament-based process	2/925	397/18723	0.999999967	0.837111134	PICK1/SPIRE1	2	1.41379E-08	0.101970182
GO:0030111	regulation of Wnt signaling pathway	1/925	328/18723	0.999999948	0.837111134	SDHAF2	1	2.26444E-08	0.061710613
GO:0043410	positive regulation of MAPK cascade	4/925	480/18723	0.999999938	0.837111134	PHB/PHB2/SOD1/PRDX2	4	2.69757E-08	0.168675676
GO:0000375	RNA splicing, via transesterification reactions	1/925	324/18723	0.999999936	0.837111134	C1QBP	1	2.7834E-08	0.062472472
GO:0032535	regulation of cellular component size	2/925	383/18723	0.999999935	0.837111134	PICK1/SPIRE1	2	2.81809E-08	0.105697551

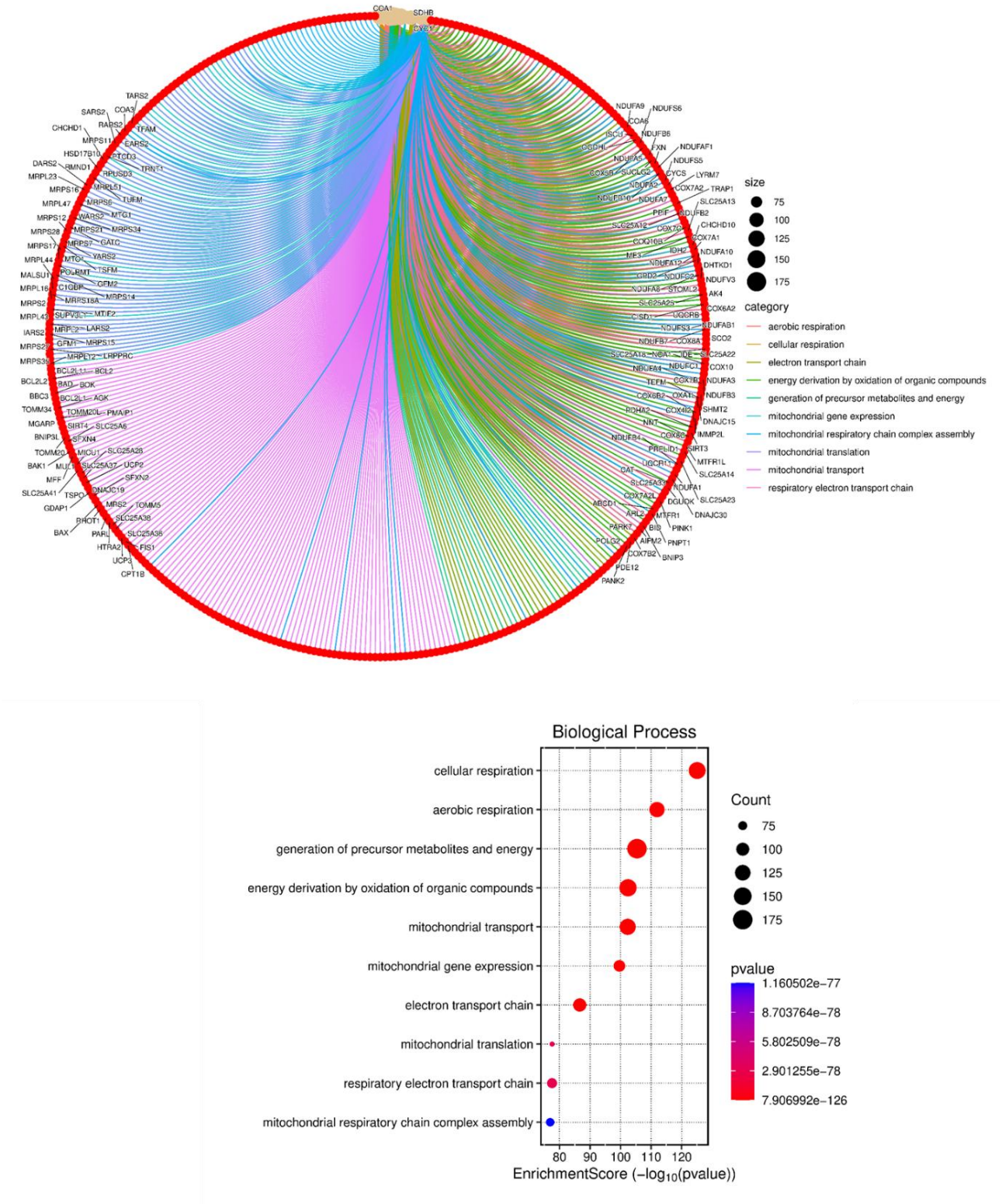

Figure 3. BP of regulated mitochondrial genes showing significant enrichment of mitochondrial bioenergetics and respiratory processes.

The CC and GO enrichment analysis demonstrated a strong and highly significant association of the analyzed gene set with mitochondrial structures, highlighting mitochondria as the primary subcellular localization of these genes. The most enriched terms included the mitochondrial inner membrane, mitochondrial matrix, and mitochondrial protein-containing complexes, with exceptionally high enrichment scores (-log10 p values ~80), indicating robust statistical significance. Enrichment of terms such as inner mitochondrial membrane protein complex, integral and intrinsic components of the mitochondrial membrane further suggests that a large proportion of these genes encode membrane-associated or membrane-embedded proteins. Additionally, the significant representation of mitochondrial ribosome and organellar ribosome categories points to a functional involvement in mitochondrial protein translation, while

enrichment of mitochondrial and organelle outer membrane terms indicates broader distribution across mitochondrial subcompartments. Collectively, these findings underscore a dominant mitochondrial localization of the gene set, supporting their potential roles in mitochondrial structure, bioenergetics, and organelle-specific metabolic and translational processes (Figure 4). The top 10 CC enrichment results revealed in Table 2.

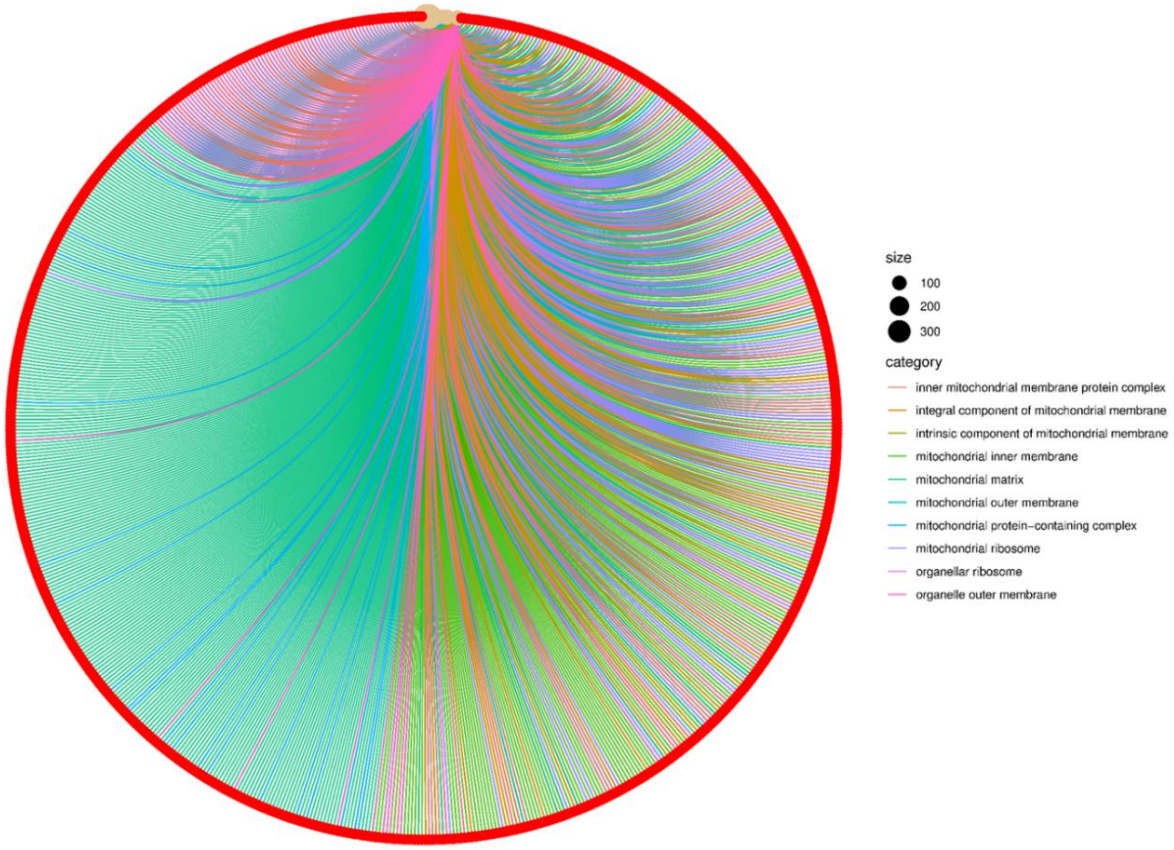

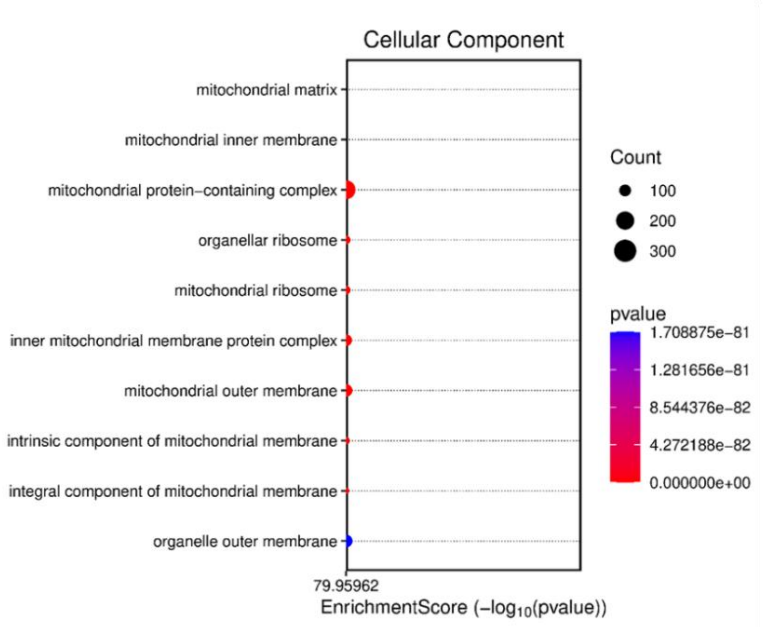

Figure 4. CC and GO enrichment analysis showing predominant localization of the gene set to mitochondrial membranes, complexes, and ribosomal structures.

Table 2. The top 10 CC enrichment results in GO.

ID	Description	Gene Ratio	Bg Ratio	P value	Qvalue	Gene ID	Count	Enrichment. Score	Fold. Enrichment
GO: 0031252	cell leading edge	1/967	422/ 19550	1	0.853395318	*THEM4*	1	1.72387E-10	0.047907977
GO: 0005667	transcription regulator complex	1/967	413/ 19550	0.999999999	0.853395318	*APEX1*	1	2.74927E-10	0.048951977
GO: 0005911	cell-cell junction	3/967	494/ 19550	0.999999996	0.853395318	*POLDIP2/TMEM65/ PARK7*	3	1.53203E-09	0.122776315
GO: 0009897	external side of plasma membrane	2/967	421/ 19550	0.99999999	0.853395318	*IDE/GSR*	2	4.25118E-09	0.096043546
GO: 0016324	apical plasma membrane	2/967	367/ 19550	0.99999986	0.853395318	*AHCYL1/ADCY10*	2	6.09734E-08	0.110175294
GO: 0000151	ubiquitin ligase complex	1/967	301/ 19550	0.999999793	0.853395318	*FBXL4*	1	8.98929E-08	0.067166666
GO: 0030135	coated vesicle	1/967	299/ 19550	0.999999771	0.853395318	*STX17*	1	9.96531E-08	0.067615941
GO: 0031253	cell projection membrane	2/967	346/ 19550	0.999999607	0.853395318	*THEM4/ SNAP29*	2	1.70536E-07	0.116862234
GO: 0030139	endocytic vesicle	2/967	336/ 19550	0.99999936	0.853395318	*RAB24/ PICK1*	2	2.77869E-07	0.120340277
GO: 0005788	endoplasmic reticulum lumen	2/967	313/ 19550	0.999998042	0.853395318	*DBI/ FKBP10*	2	8.50546E-07	0.129183172

The MF and GO enrichment analysis revealed a strong predominance of redox-related and electron transport activities within the analyzed gene set Figure 5. The most significantly enriched term was electron transfer activity, displaying the highest enrichment score and gene count, indicating a central role of these genes in cellular electron transport processes. Multiple dehydrogenase-related functions were also significantly overrepresented, including NADH dehydrogenase activity, NADH dehydrogenase (ubiquinone) activity, and NAD(P)H dehydrogenase (quinone) activity, highlighting extensive involvement in mitochondrial respiratory chain reactions and redox metabolism. Additionally, enrichment of oxidoreductase activity acting on NAD(P)H, including those utilizing quinone or related compounds as electron acceptors, further supports the dominance of OXPHOS-associated enzymatic functions. The significant representation of oxidoreduction-driven active transmembrane transporter activity suggests coupling of redox reactions with proton or electron translocation across membranes. Notably, the enrichment of structural constituent of ribosome indicates the inclusion of ribosomal proteins, reflecting a link between mitochondrial bioenergetic functions and protein synthesis machinery. Collectively, these results demonstrate that the gene set is functionally enriched for mitochondrial redox enzymes, electron transport components, and associated transport and translational activities Figure 5. The top 10 MF enrichment results revealed in Table 3.

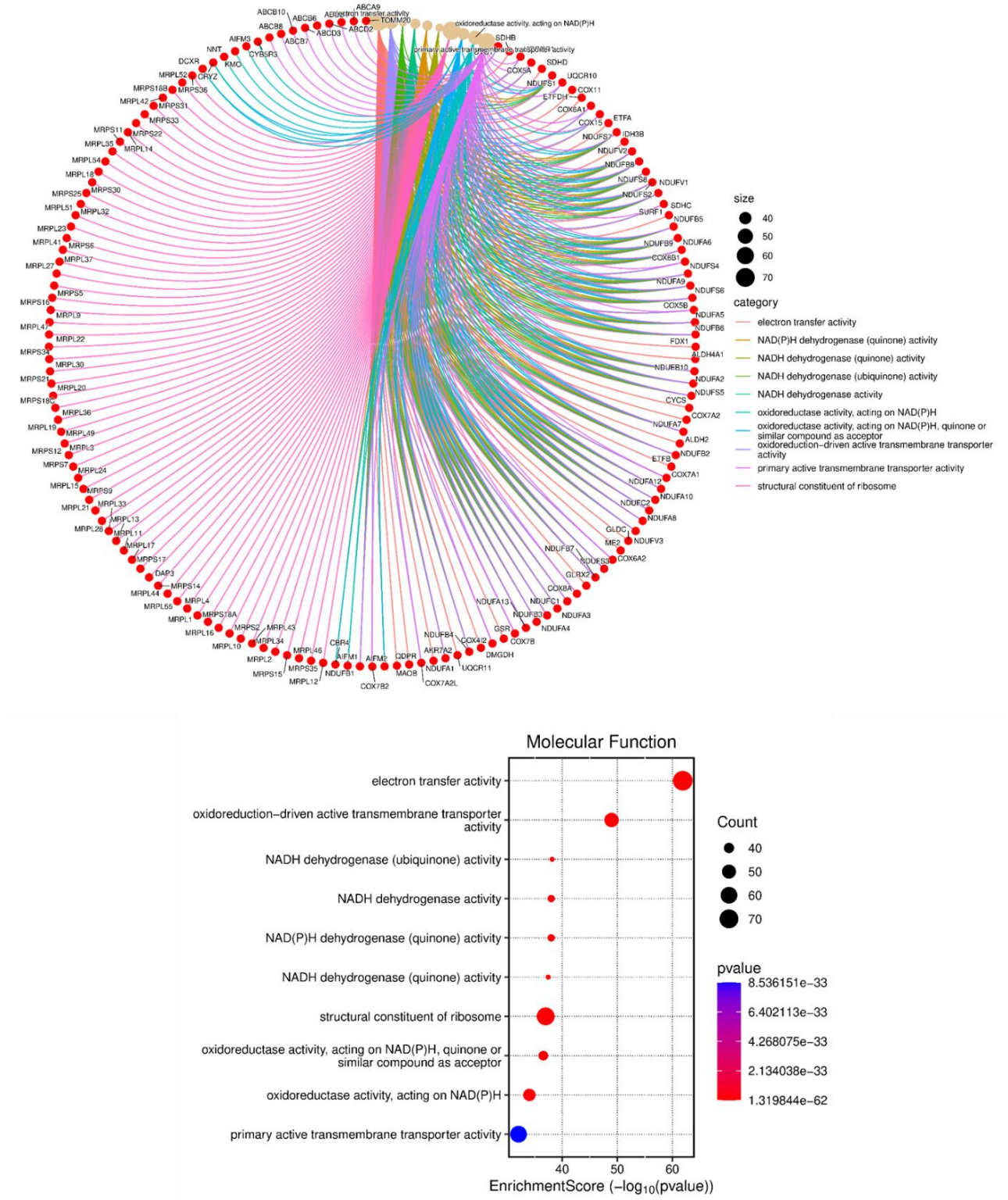

Figure 5. MF and GO enrichment analysis highlighting dominant electron transfer, oxidoreductase, and NADH dehydrogenase activities associated with mitochondrial bioenergetic processes.

Table 3. The top 10 MF enrichment results in GO.

ID	Description	Gene Ratio	Bg Ratio	P value	Q value	Gene ID	Count	Enrichment. Score	Fold. Enrichment
GO: 0019787	ubiquitin-like protein transferase activity	1/940	458/ 18368	1	0.684721513	*MUL1*	1	1.12991E-11	0.042664685
GO: 0004842	ubiquitin-protein transferase activity	1/940	433/ 18368	1	0.684721513	*MUL1*	1	4.34462E-11	0.045128004
GO: 0030546	signaling receptor activator activity	2/940	495/ 18368	1	0.684721513	*GFER/ ALKBH1*	2	4.36856E-11	0.078951214
GO: 0048018	receptor ligand activity	2/940	487/ 18368	1	0.684721513	*GFER/ ALKBH1*	2	6.62178E-11	0.080248154
GO: 0005096	GTPase activator activity	3/940	462/ 18368	0.999999993	0.684721513	*DNM1L/ PGAM5/ THG1L*	3	3.2156E-09	0.12688588
GO: 0030695	GTPase regulator activity	4/940	488/ 18368	0.999999981	0.684721513	*DNAJA3/ DNM1L/ PGAM5/ THG1L*	4	8.21915E-09	0.160167422
GO: 0060589	nucleoside-triphosphatase regulator activity	4/940	488/ 18368	0.999999981	0.684721513	*DNAJA3/ DNM1L/ PGAM5/ THG1L*	4	8.21915E-09	0.160167422
GO: 0061659	ubiquitin-like protein ligase activity	1/940	316/ 18368	0.999999947	0.684721513	*MUL1*	1	2.3133E-08	0.06183679
GO: 0061630	ubiquitin protein ligase activity	1/940	304/ 18368	0.999999899	0.684721513	*MUL1*	1	4.39364E-08	0.064277716
GO: 0003779	actin binding	4/940	441/ 18368	0.999999823	0.684721513	*MSRB2/ MYO19/ PICK1/S PIRE1*	4	7.6794E-08	0.17723742

The KEGG pathway enrichment analysis demonstrated a strong and statistically significant overrepresentation of pathways related to mitochondrial energy metabolism and systemic metabolic regulation (Figure 6). Among the top enriched pathways, thermogenesis and OXPHOS exhibited the highest enrichment scores and gene counts, indicating that a large proportion of the analyzed genes participate in mitochondrial ATP production and heat generation processes. Additional significantly enriched pathways included diabetic cardiomyopathy, non-alcoholic fatty liver disease, and carbon metabolism, suggesting a close functional association between mitochondrial dysfunction, metabolic homeostasis, and cardiometabolic disorders. The enrichment of valine, leucine, and isoleucine degradation further highlights the involvement of branched-chain amino acid metabolism, which is tightly linked to mitochondrial oxidative capacity and energy balance. The top 10 KEGG enrichment results are shown in Table 4.

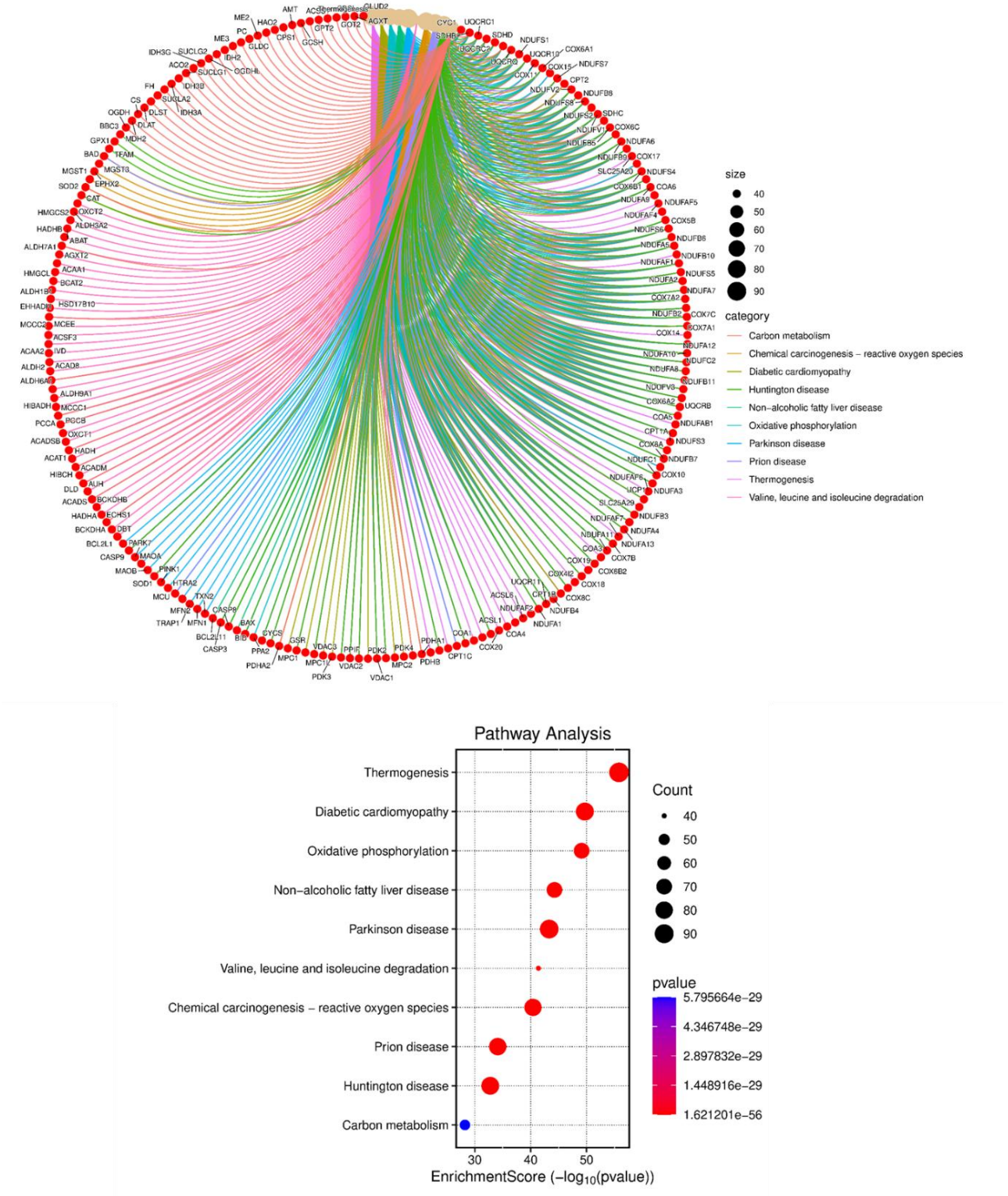

Figure 6. KEGG pathway enrichment analysis highlighting dominant mitochondrial and metabolic pathways, including thermogenesis, OXPHOS, and disease-associated energy metabolism pathways.

Table 4. The top 10 KEGG enrichment pathways based on P-value.

ID	Description	Gene Ratio	Bg Ratio	P value	P. Adjust	Q value	Gene ID	Count	Enrichment. Score	Fold. Enrichment
hsa 05210	Colorectal cancer	10/ 554	87/ 9396	0.031492843	0.10914643	0.081740617	*CYCS/BAX/BAK1/PMAIP1/CASP9/BBC3/BAD/BCL2/CASP3/BCL2L11*	10	1.501788127	1.949458484
hsa 00053	Ascorbate and aldarate metabolism	5/ 554	30/ 9396	0.029308613	0.102987209	0.077127928	*ALDH9A1/ALDH2/ALDH1B1/ALDH7A1/ALDH3A2*	5	1.533004738	2.826714801
hsa 04217	Necroptosis	16/ 554	159/ 9396	0.025117855	0.089504468	0.067030598	*AIFM1/SLC25A4/VDAC1/VDAC2/SLC25A5/VDAC3/SLC25A31/BAX/DNM1L/PGAM5/FTH1/BID/SLC25A6/GLUD2/CASP8/BCL2*	16	1.600017458	1.706695729
hsa 04922	Glucagon signaling pathway	12/ 554	107/ 9396	0.023320386	0.084286538	0.063122849	*PDHA1/PDHB/CPT1A/PDHA2/CPT1B/PCK2/ACACA/ACACB/LDHAL6B/LDHB/PRKACA/CPT1C*	12	1.632264266	1.902088465
hsa 00480	Glutathione metabolism	8/554	59/ 9396	0.021630556	0.079312038	0.059397407	*IDH2/GSTK1/GSR/LAP3/GPX1/MGST1/MGST3/GPX4*	8	1.664932322	2.299700177
hsa 01040	Biosynthesis of unsaturated fatty acids	5/554	27/ 9396	0.019181663	0.071367068	0.053447357	*HSD17B4/ACAA1/ACOT2/ACOT7/SCP2*	5	1.717113755	3.140794224
hsa 00350	Tyrosine metabolism	6/554	36/ 9396	0.017551752	0.06627751	0.049635747	*GSTZ1/FAHD1/GOT2/MAOB/MAOA/COMT*	6	1.755679537	2.826714801
hsa 00120	Primary bile acid biosynthesis	4/554	17/ 9396	0.01537847	0.058950801	0.044148717	*HSD17B4/CYP27A1/SCP2/AMACR*	4	1.813086872	3.99065619
hsa 00910	Nitrogen metabolism	4/554	17/ 9396	0.01537847	0.058950801	0.044148717	*CPS1/CA5B/CA5A/GLUD2*	4	1.813086872	3.99065619
hsa 04216	Ferroptosis	7/554	42/ 9396	0.010616663	0.041968996	0.03143091	*VDAC2/VDAC3/ACSL6/ACSL1/FTMT/FTH1/GPX4*	7	1.974011972	2.826714801

Several neurodegenerative and stress-related pathways were significantly enriched, including Parkinson disease, Huntington disease, and prion disease, reflecting the central role of mitochondrial respiratory chain components in neuronal survival and neurodegeneration. The presence of chemical carcinogenesis-reactive oxygen species (ROS) pathways underscores the contribution of these genes to redox regulation and oxidative stress responses. Detailed pathway mapping of OXPHOS revealed extensive representation of genes encoding subunits of mitochondrial respiratory chain complexes I-V, confirming their coordinated involvement in electron transport and ATP synthesis. Collectively, these findings indicate that the gene set is predominantly enriched in mitochondrial bioenergetic, metabolic, and redox-related pathways with broad relevance to metabolic, cardiovascular, and neurodegenerative diseases (Figure 7).

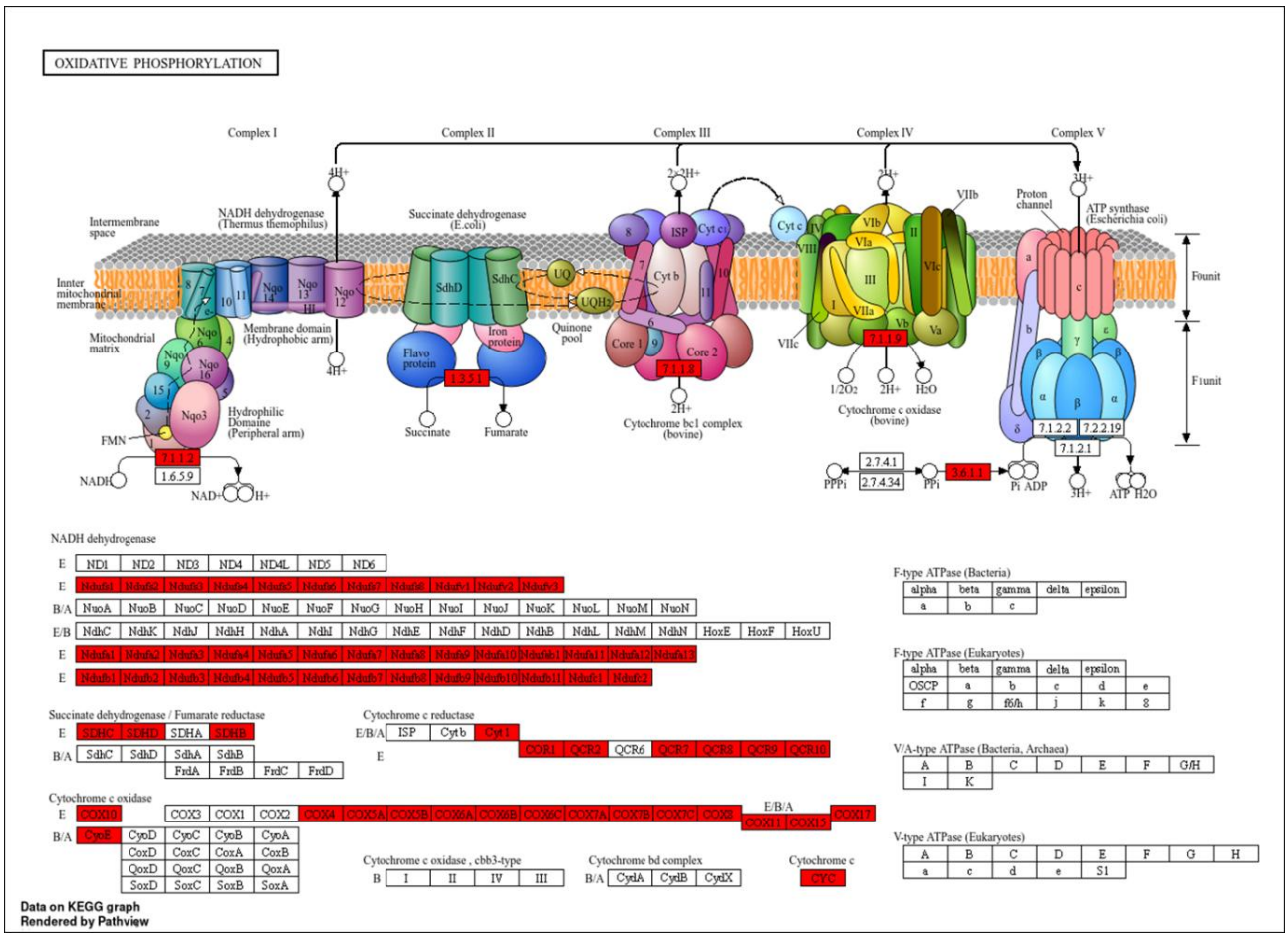

Figure 7. KEGG OXPHOS pathway map illustrating extensive involvement of the identified genes across mitochondrial respiratory chain complexes I-V.

3.5 Protein-Protein Interaction Network

To explore the functional relationships among differentially expressed mitochondrial genes, a PPI network was constructed. As shown in Figure 8A, the global PPI network revealed a highly interconnected architecture, indicating extensive functional coordination among mitochondrial proteins. The dense core of the network suggests the presence of key hub proteins with high connectivity, which are likely to play central roles in mitochondrial metabolism, bioenergetics, and protein import. Peripheral nodes showed fewer interactions, reflecting more specialized or context-dependent functions. A refined subnetwork analysis (Figure 8B) highlighted strong interaction patterns among a subset of mitochondrial proteins. Notably, proteins such as TUFM, VDAC1, NDUFAB1, CYCS, translocase of outer mitochondrial membrane (TOMM) 20, MTCH1, ETFA, SSBP1, SUCLA2, and COX18 displayed multiple interactions with one another, underscoring their coordinated involvement in mitochondrial OXPHOS, metabolite transport, and mitochondrial protein biogenesis. TUFM and VDAC1, in particular, emerged as interaction-rich nodes, suggesting their importance in maintaining mitochondrial functional integrity. Further visualization of the core interaction module (Figure 8C) emphasized the central positioning of CYCS and NDUFAB1, which showed strong connectivity with several other mitochondrial proteins. CYCS is a critical component of the ETC and apoptotic signaling, while NDUFAB1 is essential for complex I assembly and fatty acid metabolism. Their hub-like behavior supports their regulatory significance within the mitochondrial interaction network.

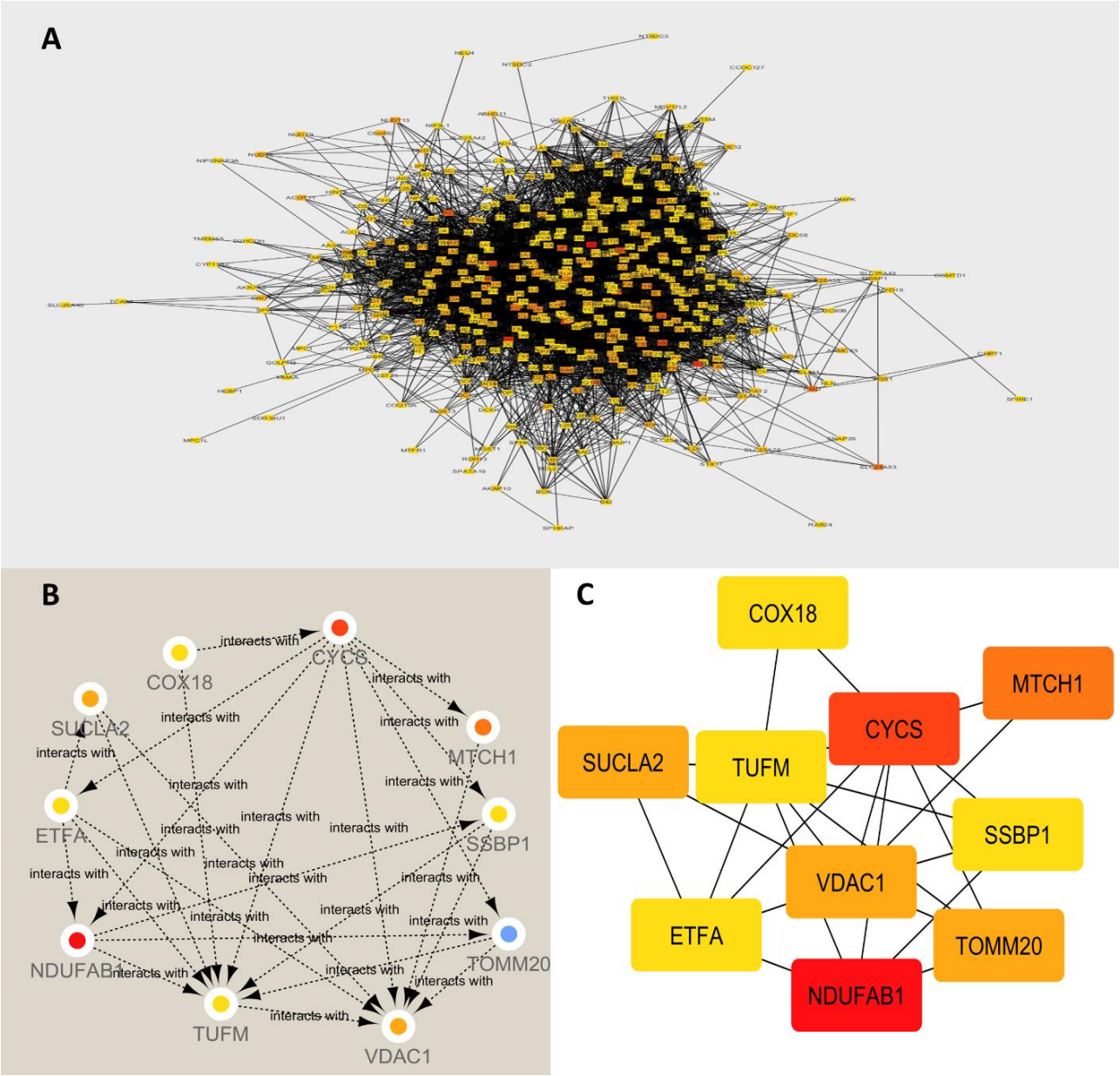

Figure 8. PPI network of highly differentially expressed mitochondrial genes, illustrating the global interaction landscape (A), a refined interaction subnetwork (B), and the prioritized core module highlighting the top 10 hub mitochondrial proteins (C).

Prioritization of key mitochondrial genes: Based on network topology parameters, including degree of connectivity and interaction density, we prioritized the top 10 highly differentially expressed mitochondrial genes: CYCS, NDUFAB1, TUFM, VDAC1, TOMM20, MTCH1, ETFA, SSBP1, SUCLA2, and COX18. These genes represent central hubs within the PPI network and are likely to have substantial functional impact on mitochondrial dynamics and energy metabolism. Their prioritization provides a focused set of candidate genes for downstream functional validation and mechanistic studies aimed at understanding mitochondrial dysregulation in the studied condition.

3.6 Genes Co-expression

Gene co-expression analysis of the prioritized mitochondrial genes revealed consistent and conserved expression relationships across species. As shown in the figure, several strong co-expression signals were observed among NDUFAB1, TUFM, CYCS, VDAC1, TOMM20, ETFA, SSBP1, MTCH1, COX18, and SUCLA2 in Homo sapiens, indicating coordinated transcriptional regulation of genes involved in mitochondrial metabolism, protein import, and OXPHOS. Importantly, these co-expression patterns were also detected in multiple non-human organisms, including mammals, plants, fungi, and bacteria, demonstrating evolutionary conservation of these gene relationships. The presence of transferred co-expression signals across diverse species suggests that these genes participate in fundamental mitochondrial and metabolic processes that are preserved across phylogeny, thereby reinforcing their functional relevance and supporting their prioritization as key mitochondrial regulators in the studied condition (Figure 9).

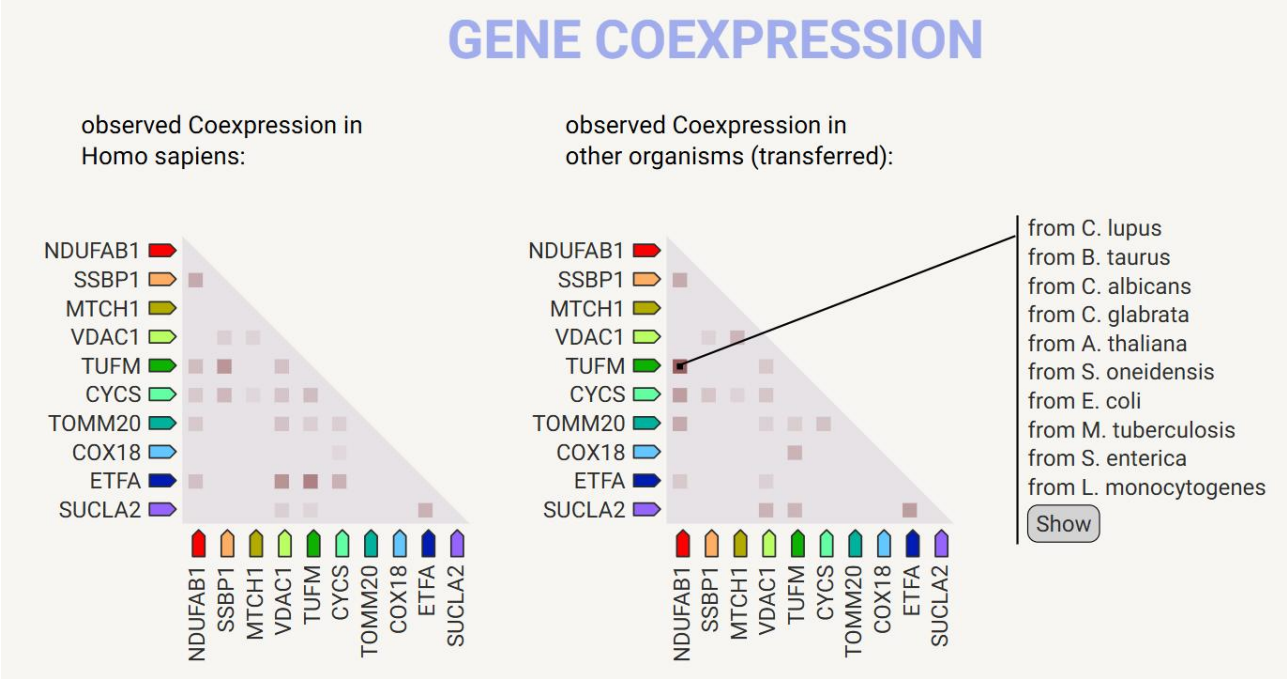

Figure 9. Gene co-expression analysis of prioritized mitochondrial genes showing observed co-expression patterns in homo sapiens and conserved co-expression relationships transferred across multiple organisms.

3.7 Integrated Network and Clustering Analysis

Integrated network clustering and interaction analysis revealed a dominant mitochondrial module comprising eight highly interconnected genes (NDUFAB1, TUFM, CYCS, VDAC1, TOMM20, ETFA, SSBP1, and SUCLA2), indicating their active and coordinated roles in mitochondrial function. As shown in the figure, these genes formed the primary cluster associated with mitochondrial nucleoid organization and metabolic regulation, characterized by dense intra-cluster connectivity and multiple shared interactions. In contrast, MTCH1 and COX18 segregated into smaller, distinct clusters with limited connectivity, suggesting more specialized or auxiliary roles. The expanded interaction network further demonstrated that the eight core mitochondrial genes act as central hubs linking multiple mitochondrial and metabolic pathways, including OXPHOS, protein import, and electron transport. Collectively, these findings support the prioritization of eight mitochondrial genes as key active regulators within the mitochondrial interaction landscape, highlighting their potential functional importance in the studied biological context (Figure 10).

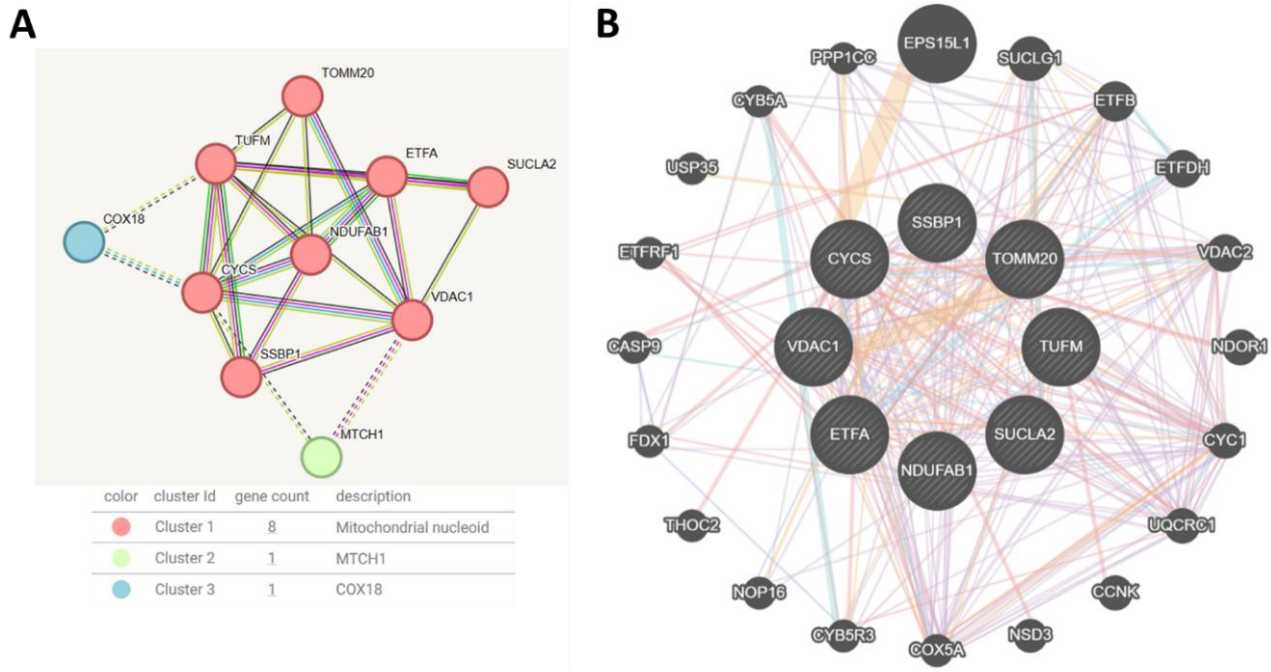

Figure 10. Network clustering and interaction analysis highlighting eight prioritized mitochondrial hub genes forming a highly interconnected core module, with MTCH1 and COX18 represented as distinct peripheral clusters.

3.8 Transcriptomic Factor and Drug Therapeutics

The transcriptomic factor analysis reveals that the gene signature is predominantly regulated by PRDM2, MLX, E2F4, and HMGN3, supported by strong co-expression and multi-source ChIP-seq evidence, indicating a coordinated transcriptional and chromatin-level regulatory network. (Figure 11A) (Transcriptomic factors) demonstrates that the gene signature is primarily regulated by a defined transcriptional network, with PRDM2, MLX, E2F4, and HMGN3 showing the strongest enrichment supported by co-expression (ARCHS4, GTEx) and multiple ChIP-seq datasets (ENCODE, ReMap, literature), indicating robust transcriptional and chromatin-associated control. (Figure 11B) (DrugMatrix) identifies compounds such as aceclofenac, azathioprine, minoxidil, flutamide, busulfan, neomycin, lead acetate, bezafibrate, and methyl salicylate whose *in vivo* rat tissue expression profiles significantly overlap with the transcriptomic signature, suggesting potential pharmacological modulation of the same regulatory pathways. (Figure 11C) (Proteomics Drug Atlas 2023) further supports these findings at the protein level, highlighting drugs including indapamide, dapagliflozin, rofecoxib, varespladib, and epristeride that induce concordant up- or down-regulation patterns, confirming target engagement beyond transcription. (Figure 11D) (Sciplex Drug Perturbation Signatures 2025) extends this evidence to single-cell perturbation contexts, where agents such as busulfan, triamcinolone acetonide, pirarubicin, thalidomide, quercetin, and AMG-900 elicit consistent up- or down-regulated responses across multiple cell lines. Together, these analyses clearly demonstrate a convergence between key transcriptomic regulators and actionable drug targets, underscoring a coherent regulatory-pharmacological axis underlying the observed molecular phenotype.

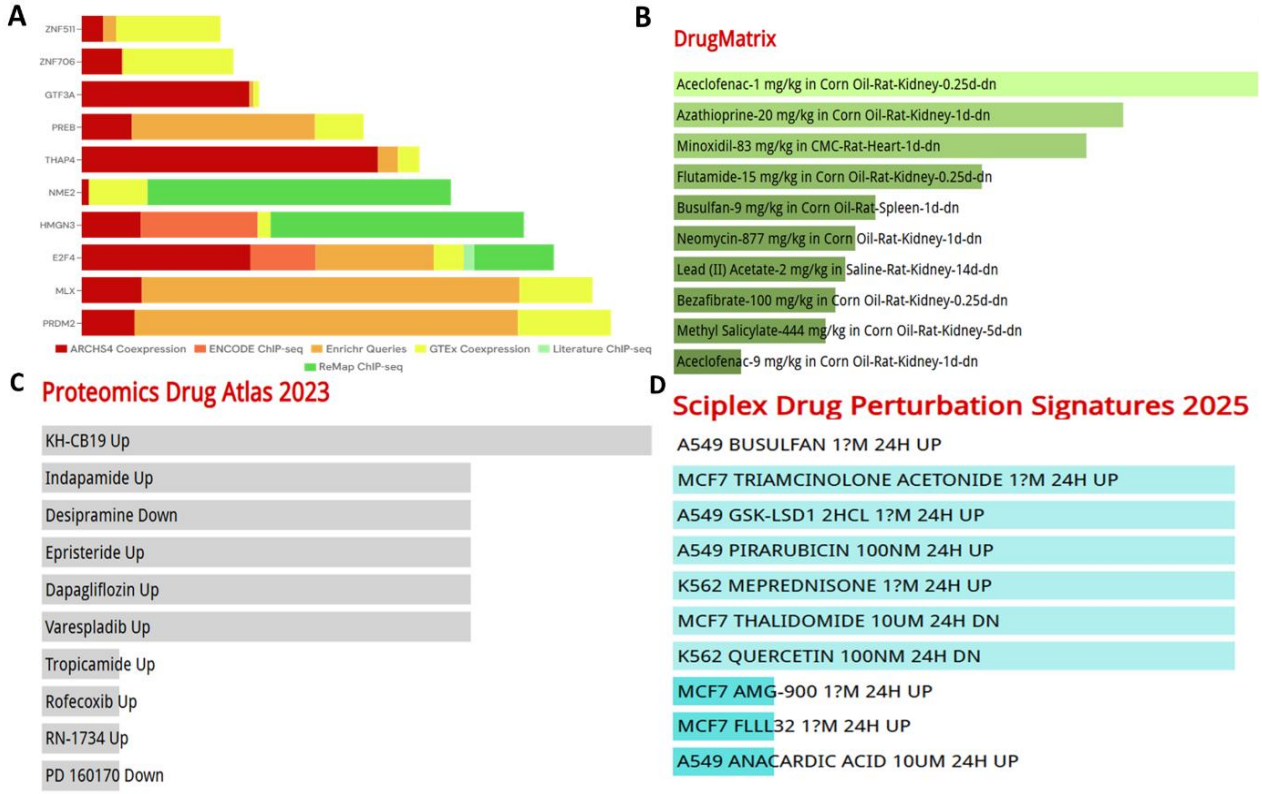

Figure 11. Integrated transcriptomic factor and drug perturbation analysis identifying key regulatory TF and convergent pharmacological signatures across DrugMatrix, proteomics drug atlas, and sciplex datasets.

3.9 Survival and Prognostic Analysis

Across the evaluated lung adenocarcinoma cohorts, most of the mitochondrial and metabolic genes tested showed statistically significant associations with overall survival when stratified by median expression. NDUFAB1, SSBP1, VDAC1, TUFM, and CYCS demonstrated significant prognostic value, with SSBP1, TUFM, and CYCS yielding the strongest signals based on highly significant P values ($4.7e^{-5}$, $5.1e^{-11}$, and $3.1e^{-9}$, respectively). For TUFM and CYCS, high expression correlated with substantially longer median survival compared to their low-expression cohorts, while NDUFAB1, SSBP1, and VDAC1 showed the opposite pattern, with high expression associated with shorter survival. TOMM20, ETFA, and SUCLA2 did not reach statistical significance. Based on comparative prognostic performance, significance, and consistency of survival differences, we selected three genes as biomarkers for adenocarcinoma (Figure 12) (Table 5).

Table 5. Prognostic performance of candidate mitochondrial and metabolic genes in lung adenocarcinoma based on Kaplan-Meier overall survival analysis.

Affy ID	Gene	P value	Median Survival (Low exp., months)	Median Survival (High exp., months)	Significant (P < 0.05)
202077_at	NDUFAB1	0.0261	74	63	Yes
202591_s_at	SSBP1	4.7E-5	80	57	Yes
212038_s_at	VDAC1	0.0033	80	57	Yes
238190_at	TUFM	5.1E-11	52	99.43	Yes
229415_at	CYCS	3.1E-9	52.97	102	Yes
200662_s_at	TOMM20	0.1377	66.47	73.3	No
201931_at	ETFA	0.569	71	67	No
202930_s_at	SUCLA2	0.346	68.7	71	No

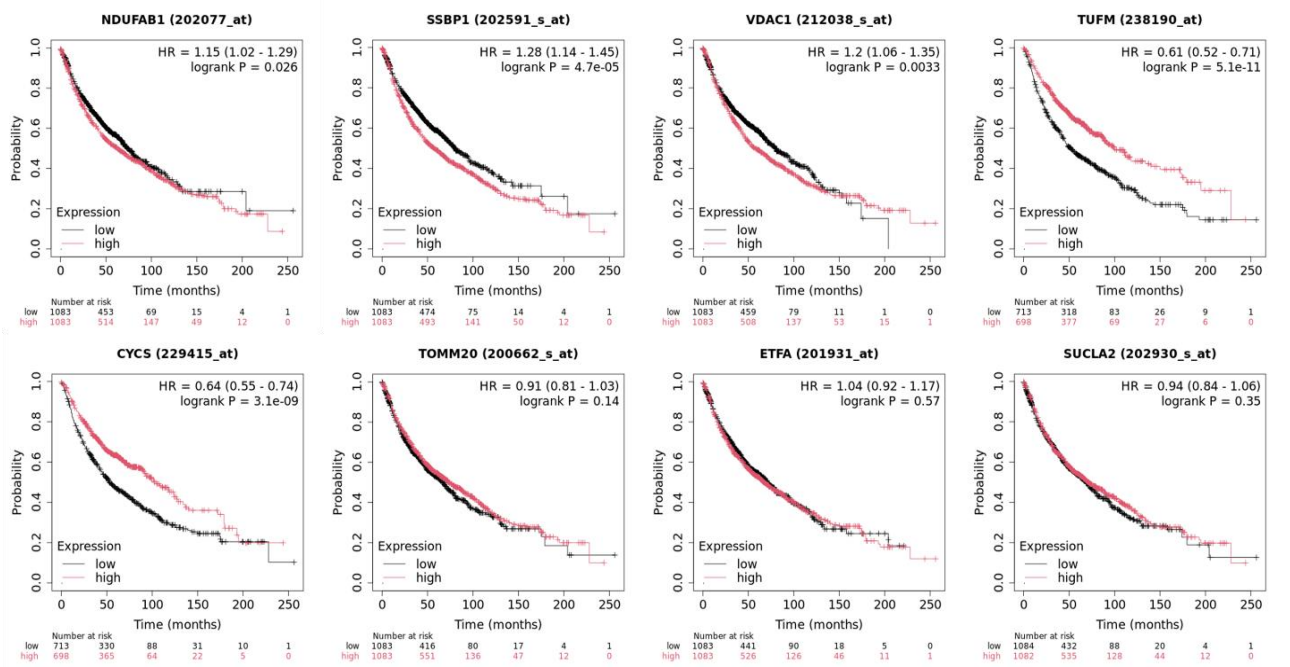

Figure 12. Prognostic significance of DE-MGs in adenocarcinoma based on kaplan-meier plotter analysis.

4. Discussion

Lung adenocarcinoma represents the most prevalent histological subtype of NSCLC and is characterized by profound molecular heterogeneity, metabolic reprogramming, and strong dependence on mitochondrial function to support tumor growth and survival [25]. Increasing evidence indicates that mitochondrial bioenergetics, redox balance, and apoptotic regulation play decisive roles in adenocarcinoma progression, metastatic potential, and therapeutic resistance. In this context, the present study provides a comprehensive transcriptomic and systems-level analysis demonstrating that modulation of LCRMP-1 expression is tightly associated with widespread mitochondrial gene dysregulation in lung adenocarcinoma cells [26]. The identification of a large subset of differentially expressed mitochondrial genes highlights mitochondria as a central hub linking LCRMP-1-driven transcriptional programs to adenocarcinoma pathobiology, reinforcing the concept that mitochondrial remodeling is a defining feature of this cancer subtype [4].

Our differential expression analyses revealed robust and reciprocal transcriptional changes following LCRMP-1 overexpression and silencing, supporting a regulatory role for LCRMP-1 in shaping pro-tumorigenic gene programs. The enrichment of mitochondrial genes among the differentially expressed set suggests that LCRMP-1 influences not only cytoskeletal dynamics and invasion, as previously reported, but also core metabolic and bioenergetic processes. This observation aligns with emerging models of cancer metabolism in which oncogenic signals rewire mitochondrial function to meet increased energetic and biosynthetic demands [27]. The consistent enrichment of pathways related to OXPHOS, cellular respiration, and ETC activity underscores a coordinated alteration of mitochondrial energy production in lung adenocarcinoma cells. Functional enrichment analyses further demonstrated that the regulated mitochondrial genes are predominantly localized to the mitochondrial inner membrane, matrix, and respiratory chain complexes, emphasizing their direct involvement in ATP generation and redox regulation. The strong representation of oxidoreductase and NADH dehydrogenase activities indicates enhanced modulation of electron flow and ROS handling, processes that are critical for maintaining tumor cell viability while avoiding excessive oxidative stress. These findings support the notion that lung adenocarcinoma cells fine-tune mitochondrial respiration rather than simply suppressing it,

consistent with growing evidence that functional OXPHOS remains essential in many solid tumors. Network-based analyses identified a tightly connected core of mitochondrial hub genes, including CYCS, NDUFAB1, TUFM, VDAC1, TOMM20, ETFA, SSBP1, and SUCLA2, suggesting that these genes act in concert to maintain mitochondrial integrity and metabolic flux [28]. The central positioning of CYCS and NDUFAB1 within the PPI network highlights a dual role for mitochondria in both energy metabolism and apoptotic signaling. Such duality is particularly relevant in adenocarcinoma, where evasion of apoptosis and metabolic flexibility jointly contribute to aggressive tumor behavior [25]. The strong evolutionary conservation of co-expression patterns among these genes further underscores their fundamental biological importance and supports their relevance beyond a single experimental system. Importantly, the integration of transcriptomic factor analysis identified PRDM2, MLX, E2F4, and HMGN3 as key upstream regulators of the mitochondrial gene signature. These factors are known to participate in chromatin remodeling, cell-cycle control, and metabolic regulation, providing a mechanistic link between transcriptional control and mitochondrial reprogramming in lung adenocarcinoma [29]. The convergence of TF enrichment with drug perturbation signatures suggests that the identified mitochondrial network is pharmacologically tractable. Compounds highlighted across DrugMatrix, proteomic, and single-cell perturbation datasets may therefore represent candidates for repurposing or combination strategies aimed at targeting mitochondrial vulnerabilities in adenocarcinoma [30].

Survival analyses demonstrated that several prioritized mitochondrial genes possess significant prognostic value in lung adenocarcinoma patients. Notably, differential expression of TUFM and CYCS was associated with markedly altered overall survival, indicating that mitochondrial translation and apoptotic competence may influence clinical outcomes. The opposing prognostic trends observed for genes such as NDUFAB1, SSBP1, and VDAC1 further reflect the complex, context-dependent roles of mitochondrial pathways in tumor progression. These findings position mitochondrial gene signatures not only as mechanistic drivers of adenocarcinoma biology but also as potential biomarkers and therapeutic targets. While further experimental validation and clinical studies are warranted, this integrative analysis provides a strong foundation for understanding how LCRMP-1-associated mitochondrial reprogramming contributes to lung adenocarcinoma pathogenesis and patient prognosis.

Our study provides a comprehensive molecular and systems-level analysis of LCRMP-1-associated mitochondrial remodeling, we acknowledge that these findings are primarily hypothesis-generating from a clinical perspective. Translating these insights into patient care will require further validation in independent cohorts, functional assays to confirm the role of mitochondrial hub genes, and exploration of biomarker-driven trial designs. By explicitly framing our results in this context, we aim to guide future studies toward actionable experimental and translational steps without overextending the current preclinical and computational evidence.

5. Conclusion

This study demonstrates that LCRMP-1-associated transcriptomic alterations in lung adenocarcinoma are strongly linked to mitochondrial reprogramming, particularly affecting bioenergetic, metabolic, and redox pathways. The identification of key mitochondrial hub genes with prognostic significance highlights mitochondria as central regulators of tumor progression and potential therapeutic vulnerability. Collectively, these findings provide a systems-level framework for understanding mitochondrial dysregulation in lung adenocarcinoma and support the development of mitochondria-focused biomarkers and targeted interventions.

6. Future Direction

Building on the findings of this study, several avenues for future research can be envisioned to bridge the gap between preclinical insights and clinical application. First, the mitochondrial hub genes identified in our analyses such as TUFM, CYCS, and NDUFAB1 hold potential as prognostic biomarkers for patient stratification. Future studies should aim to validate these genes in independent patient cohorts, assessing their capacity to distinguish subgroups with distinct metabolic profiles, therapeutic vulnerabilities, or predicted clinical outcomes. Integrating these mitochondrial signatures into patient stratification frameworks could enhance precision oncology approaches and guide individualized treatment strategies in lung adenocarcinoma.

Second, our drug perturbation analyses provide a roadmap for translational exploration of compounds that modulate the LCRMP-1-mitochondrial network. Preclinical evaluation of these agents, alone or in combination with existing therapies, could identify metabolically targeted interventions with enhanced efficacy. Additionally, incorporating mitochondrial gene signatures into early-phase clinical trial designs as exploratory biomarkers, inclusion criteria, or surrogate endpoints may facilitate the assessment of metabolic response, therapeutic susceptibility, and patient outcomes. Together, these strategies provide actionable hypotheses for leveraging mitochondrial bioenergetic remodeling in clinical decision-making, while acknowledging the need for further experimental validation to ensure safety, efficacy, and reproducibility.

Abbreviations

AJCC: American joint committee on cancer

ARCHS4: All RNA-seq and ChIP-seq sample and signature search

BP: Biological Process

ChIP-seq: Chromatin immunoprecipitation sequencing

CL1-0: Human lung adenocarcinoma cell line CL1-0

CL1-5: Human lung adenocarcinoma cell line CL1-5

CC: Cellular Component

DEGs: Differentially expressed genes

ENCODE: Encyclopedia of DNA elements

ETC: Electron transport chain

FDR: False discovery rate

GEO: Gene expression omnibus

GTEx: Genotype-tissue expression

KEGG: Kyoto encyclopedia of genes and genomes

LCRMP-1: Long-form collapsin response mediator protein-1

MA plot: Mean-difference plot

MF: Molecular function

NSCLC: Non-small cell lung cancer

OXPHOS: Oxidative phosphorylation

PPI: Protein-protein interaction

ROS: Reactive oxygen species

TF: Transcription factor

TOMM: Translocase of outer mitochondrial membrane

Gene Symbols (HGNC-approved)

CYCS: Cytochrome c, somatic

ETFA: Electron transfer flavoprotein subunit alpha

MTCH1: Mitochondrial carrier 1

NDUFAB1: NADH: Ubiquinone oxidoreductase subunit AB1

SSBP1: Single-stranded DNA binding protein 1

SUCLA2: Succinate-CoA ligase ADP-forming beta subunit

TUFM: Tu Translation elongation factor, mitochondrial

VDAC1: Voltage-dependent anion channel 1

Conflict of Interest

The authors declare no conflict of interest in this research article.

Generative AI Statement

The authors declare that no Gen AI was used in the creation of this manuscript.

References

[1] Hendriks LEL, Remon J, Faivre-Finn C, Garassino MC, Heymach JV, Kerr KM, et al. Non-small-cell lung cancer. Nature Reviews. Disease Primers, 2024, 10(1), 71. DOI: 10.1038/s41572-024-00551-9

[2] Mir SA, Dar A, Hamid L, Nisar N, Malik JA, Ali T, et al. Flavonoids as promising molecules in the cancer therapy: An insight. Current Research in Pharmacology and Drug Discovery, 2024, 6, 100167. DOI: 10.1016/j.crphar.2023.100167

[3] Khacho M, Harris R, Slack RS. Mitochondria as central regulators of neural stem cell fate and cognitive function. Nature Reviews Neuroscience, 2019, 20, 34-48. DOI: 10.1038/s41583-018-0091-3
[4] Hsu YL, Hung PF, Wang CC, Chang YL, Wu CT, Wu PS, et al. LCRMP-1 induces tumor angiogenesis by transcriptionally upregulating SERPINE1 in lung adenocarcinoma. Communications Biology, 2025, 8, 1676. DOI: 10.1038/s42003-025-09071-y
[5] Yu YF, Yan R, Chen XZ, Sun T, Yan JF. Paeonol suppresses the effect of ox-LDL on mice vascular endothelial cells by regulating miR-338-3p/TET2 axis in atherosclerosis. Molecular and Cellular Biochemistry, 2020, 475(1-2), 127-135. DOI: 10.1007/s11010-020-03865-w
[6] Yan XH, Qi M, Li PF, Zhan YH, Shao HJ. Apigenin in cancer therapy: Anti-cancer effects and mechanisms of action. Cell and Bioscience, 2017, 7, 50. DOI: 10.1186/s13578-017-0179-x
[7] Kanehisa M, Goto S. KEGG: Kyoto encyclopedia of genes and genomes. Nucleic Acids Research, 2000, 28(1), 27-30. DOI: 10.1093/nar/28.1.27
[8] Barrett T, Wilhite SE, Ledoux P, Evangelista C, Kim IF, Tomashevsky M, et al. NCBI GEO: Archive for functional genomics data sets -- update. Nucleic Acids Research, 2013, 41, D991-D995. DOI: 10.1093/nar/gks1193
[9] Chinnery PF, Hudson G. Mitochondrial genetics. British Medical Bulletin, 2013, 106(1), 135-159. DOI: 10.1093/bmb/ldt017
[10] Zhou T, Yao J, Liu ZJ. Gene ontology, enrichment analysis, and pathway analysis. Bioinformatics in Aquaculture: Principles and Methods, 2017, 150-168. DOI: 10.1002/9781118782392.ch10
[11] Vilgelm AE, Johnson DB, Richmond A. Combinatorial approach to cancer immunotherapy: strength in numbers. Journal of Leukocyte Biology, 2016, 100(2), 275-290. DOI: 10.1189/jlb.5RI0116-013RR
[12] Aiman S, Ahmad A, Khan AA, Alanazi AM, Samad A, Ali SL, et al. Vaccinomics-based next-generation multi-epitope chimeric vaccine models prediction against Leishmania tropica-A hierarchical subtractive proteomics and immunoinformatics approach. Frontiers in Immunology, 2023, 14, 1259612. DOI: 10.3389/fimmu.2023.1259612
[13] Ugbaja SC, Mtambo SE, Mushebenge AG, Appiah-Kubi P, Abubakar BH, Ntuli ML, et al. Structural investigations and binding mechanisms of oseltamivir drug resistance conferred by the E119V mutation in influenza H7N9 virus. Molecules, 2022, 27(14), 4376. DOI: 10.3390/molecules27144376
[14] Pertea M, Pertea GM, Antonescu CM, Chang TC, Mendell JT, Salzberg SL. StringTie enables improved reconstruction of a transcriptome from RNA-seq reads. Nature Biotechnology, 2015, 33(3), 290-295. DOI: 10.1038/nbt.3122
[15] Hu YF, Zeng N, Ge YQ, Wang D, Qin XX, Zhang WS, et al. Identification of the shared gene signatures and biological mechanism in type 2 diabetes and pancreatic cancer. Frontiers in Endocrinology, 2022, 13, 847760. DOI: 10.3389/fendo.2022.847760
[16] Kielich N, Mazur O, Musidlak O, Gracz-Bernaciak J, Nawrot R. Herbgenomics meets Papaveraceae: A promising -omics perspective on medicinal plant research. Briefings in Functional Genomics, 2024, 23(5), 579-594. DOI: 10.1093/bfgp/elad050
[17] Szklarczyk D, Gable AL, Lyon D, Junge A, Wyder S, Huerta-Cepas J, et al. STRING v11: Protein-protein association networks with increased coverage, supporting functional discovery in genome-wide experimental datasets. Nucleic Acids Research, 2019, 47(D1), D607-D613. DOI: 10.1093/nar/gky1131
[18] Svoboda DL, Saddler T, Auerbach SS. An overview of national toxicology program's toxicogenomic applications: DrugMatrix and ToxFX. Advances in Computational Toxicology, 2019, 141-157. DOI: 10.1007/978-3-030-16443-0_8
[19] Zwyea S, Naji L, Almansouri S. Kaplan-Meier plotter data analysis model in early prognosis of pancreatic cancer. Journal of Physics: Conference Series, 2021, 12033. DOI: 10.1088/1742-6596/1853/1/012033
[20] Suresh S, Freedman A, Adams M, Hirsch E, Ernst LM. Placental histology for targeted risk assessment of recurrent spontaneous preterm birth. American Journal of Obstetrics and Gynecology, 2024, 230(4), 452.e1-452.e11. DOI: 10.1016/j.ajog.2023.09.018
[21] Ranstam J, Cook JA. Kaplan-meier curve. The British Journal of Surgery, 2017, 104(4), 442. DOI: 10.1002/bjs.10238
[22] Baru Venkata R, Prasanth DSNBK, Pasala PK, Panda SP, Tatipamula VB, Mulukuri S, et al. Utilizing andrographis paniculata leaves and roots by effective usage of the bioactive andrographolide and its nanodelivery: Investigation of antikindling and antioxidant activities through in silico and *in vivo* studies. Frontiers in Nutrition, 2023, 10, 1185236. DOI: 10.3389/fnut.2023.1185236
[23] Li J, Cao F, Yin HL, Huang ZJ, Lin ZT, Mao N, et al. Ferroptosis: Past, present and future. Cell Death and Disease, 2020, 11(2), 88. DOI: 10.1038/s41419-020-2298-2
[24] Cesari M, Fielding RA, Pahor M, Goodpaster B, Hellerstein M, Kan GAV, et al. Biomarkers of sarcopenia in clinical trials-recommendations from the international working group on sarcopenia. Journal of Cachexia, Sarcopenia and Muscle, 2012, 3(3), 181-190. DOI: 10.1007/s13539-012-0078-2
[25] Villarroel-Espindola F, Yu XQ, Datar I, Mani N, Sanmamed M, Velcheti V, et al. Spatially resolved and quantitative analysis of VISTA/PD-1H as a novel immunotherapy target in human non-small cell lung cancer. Clinical Cancer Research, 2018, 24(7), 1562-1573. DOI: 10.1158/1078-0432.CCR-17-2542
[26] Liu L, Koike H, Ono T, Hayashi S, Kudo F, Kaneda A, et al. Identification of a KLF5-dependent program and drug development for skeletal muscle atrophy. Proceedings of the National Academy of Sciences of the United States of America, 2021, 118(35), e2102895118. DOI: 10.1073/pnas.2102895118
[27] Sun H, Sun C, Xiao W. Expression regulation of co-inhibitory molecules on human natural killer cells in response to cytokine stimulations. Cytokine, 2014, 65(1), 33-41. DOI: 10.1016/j.cyto.2013.09.016
[28] Li RR, Ren T, Zeng JQ. Mitochondrial coenzyme Q protects sepsis-induced acute lung injury by activating PI3K/Akt/GSK-3β/mTOR pathway in rats. BioMed Research International, 2019, 5240898. DOI: 10.1155/2019/5240898
[29] Issahaku AR, Salifu EY, Agoni C, Alahmdi MI. Discovery of potential KRAS-SOS1 inhibitors from south african natural compounds: An *in silico* approach. ChemistrySelect, 2023, 8(24), 1-14. DOI: 10.1002/slct.202300277
[30] Zhang WT, Zeng Y, Jiao M, Ye CJ, Li YR, Liu CG, et al. Integration of high-throughput omics technologies in medicinal plant research: The new era of natural drug discovery. Frontiers in Plant Science, 2023, 14, 1073848. DOI: 10.3389/fpls.2023.1073848